Quantifying and simulating carbon and nitrogen mineralization from diverse exogenous organic matters

Florent Levavasseur, Gwenaëlle Lashermes, Bruno Mary, Thierry Morvan, Bernard Nicolardot, Virginie Parnaudeau, Laurent Thuriès, Sabine Houot

This is an Accepted Manuscript of an article published by Wiley in Soil Use and Management on 21 July 2021, available at: https://doi.org/10.1111/sum.12745

Quantifying and simulating carbon and nitrogen mineralization from diverse exogenous organic matters

F. LEVAVASSEUR [a,*], G. LASHERMES [b], B. MARY [c], T. MORVAN [d], B. NICOLARDOT [e], V. PARNAUDEAU [d], L. THURIÈS [g], S. HOUOT [a]

[a] *INRAE, AgroParisTech, Université Paris-Saclay, UMR ECOSYS, 78850 Thiverval-Grignon, France*

[b] *Université de Reims Champagne Ardenne, INRAE, FARE, UMR A 614, 51097 Reims, France*

[c] *BioEcoAgro Joint Research Unit, INRAE, Université de Liège, Université de Lille, Université de Picardie Jules Verne, 02000 Barenton-Bugny, France*

[d] *UMR SAS, INRAE, Institut Agro, 35000 Rennes, France*

[e] *Agroécologie, AgroSup Dijon, INRAE, Univ. Bourgogne, Univ. Bourgogne Franche Comté, 21000 Dijon, France*

[g] *CIRAD, UPR Recyclage et Risque, F-97743 Saint-Denis, Réunion, France, Recyclage et Risque, Univ Montpellier, CIRAD, Montpellier*

***Corresponding Author:** Florent Levavasseur. (E-mail: florent.levavasseur@inrae.fr).

Running Title: C and N mineralization from EOM

Abstract

The potential contributions of exogenous organic matters (EOMs) to soil organic C and mineral N supply depend on their C and N mineralization, which can be assessed in laboratory incubations. Such incubations are essential to calibrate decomposition models, because not all EOMs can be tested in the field. However, EOM incubations are resource-intensive. Therefore, easily measurable EOM characteristics that can be useful to predict EOM behavior are needed.

We quantified C and N mineralization during the incubation of 663 EOMs from five groups (animal manures, composts, sewage sludges, digestates, and others). This represents one of the largest and diversified set of EOM incubations. The C and N mineralization varied widely between and within EOM subgroups. We simulated C and N mineralization with a simple generic decomposition model. Three calibration methods were compared. Individual EOM calibration of the model yielded good model performances, while the use of a unique parameter set per EOM subgroup decreased the model performance, and the use of two EOM characteristics to estimate model parameters gave an intermediate model performance (average RMSE-C values of 32, 99 and 65 mg C g^{-1} added C and average RMSE-N values of 50, 126 and 110 mg N g^{-1} added N, respectively).

Because of the EOM variability, individual EOM calibration based on incubation remains the recommended method for predicting most accurately the C and N mineralization of EOMs. However, the two alternative calibration methods are sufficient for the simulation of EOMs without incubation data to obtain reasonable model performances.

Keywords: organic amendment, fertilizer, model, organic matter, soil, decomposition, N mineralization

Highlights:

- C and N mineralization in 663 exogenous organic matters was quantified under controlled conditions
- C and N mineralization varied widely between and among the subgroups of exogenous organic matters
- A simple generic model can predict the variability in C and N mineralization from EOMs
- A calibration was proposed for 26 EOM subgroups using their biochemical characteristics.

1 Introduction

Exogenous organic matter (EOM) is characterized as various residual organic matters applied to soil as organic fertilizers or organic amendments. They encompass animal manures and urban and industrial organic wastes and can be used raw or after treatments (e.g., composting or anaerobic digestion). The contribution of EOM carbon (C) to soil organic carbon (SOC) and EOM nitrogen (N) to the mineral N supply available to crops has been extensively studied, especially in long-term field experiments (Gerzabek et al., 1997; Gómez-Muñoz et al., 2017). A better characterization of the large diversity of EOM is however needed to better quantify their potential for soil carbon storage, especially EOMs that have been submitted to treatments such as composting or anaerobic digestion (Chenu et al., 2019). Due to the limited number of EOMs, cropping systems, and climate and soil conditions that can be tested *in situ*, many authors have used EOM incubations to quantify the C and N mineralization of EOMs in soil under controlled conditions (Lazicki et al., 2020; Mondini et al., 2017; Noirot-Cosson et al., 2017). The kinetics obtained during laboratory incubations can be used to predict C and N mineralization in field or greenhouse conditions with additional accounting for the effect of environmental factors (soil temperature, water content, etc.) (Delin et al., 2012; Gale et al., 2006; Pinto et al., 2020).

However, a comparison of the C and N mineralization kinetics of a wide range of common types of EOM, integrating their variability, is still lacking. EOM incubations can also be used to calibrate EOM decomposition modules in soil-crop models (Noirot-Cosson et al., 2016), which allows us to predict the impact of EOM applications under field conditions. Calibrations for many EOMs have yet to be proposed for the decomposition modules of soil-crop models, which often do not consider the diversity of and variability in EOMs. Due to the workload involved in laboratory incubations (several months of incubation are needed), the use of easily available EOM characteristics (e.g. biochemical fractions and C:N ratios) to predict C and N mineralization should be encouraged (Delin et al., 2012; Lashermes et al., 2009, 2010; Lazicki et al., 2020; Morvan & Nicolardot, 2009; Pansu & Thuriès, 2003; Parnaudeau et al., 2004). The use of these characteristics for calibrating decomposition modules in soil-crop models should allow prediction not only of the final mineralization but also the mineralization dynamics; therefore, they need to be validated for a wide range of EOMs.

The aim of this work was to quantify the C and N mineralization of a wide range of EOMs during laboratory incubations, to test the ability of a simple generic decomposition model to simulate their C and N mineralization, and to propose some simple calibration methods of the model in order to avoid the use of long and costly laboratory incubations.

2 Materials and methods

2.1 EOM database

The EOM database compiles the results of 663 EOM incubations in soil over at least 90 days under controlled laboratory conditions. The EOM incubations were performed in various research projects for many years and were not all conducted with exactly the same procedure. However, most incubations were carried out according to a standard method

(AFNOR, 2009): the equivalent of 25 g of dry soil was mixed with the EOM added at a rate corresponding to 2 g organic C kg^{-1} dry soil. The EOM was dried and ground to a particle size of 1 mm. Mineral N was added in excess to avoid any mineral N deficiency, which could have limited the EOM decomposition rate, and to highlight the potential N immobilization (Recous et al., 1995). The temperature was maintained at 28°C, and the gravimetric water content was equivalent to the field capacity (pF = 2.5). A few incubations were performed under different conditions (e.g., a temperature of 15°C and a longer duration and/or with the addition of fresh EOM) (Table S1, Appendix B, online supporting information). Most soils used in the incubations were loamy and noncalcareous with a low carbon content (mean soil carbon content equal to 11.6 g kg^{-1}, mean soil organic C:N equal to 9.8) (Table S2, Appendix B, online supporting information).

In each incubation, the CO_2 evolved and the soil mineral N were measured to determine the mineralized C and N. The net C and N mineralized from each EOM were computed by subtracting the mineralized C and N of an unamended soil (control). The proportions of the net mineralized C and N from the EOMs were obtained by dividing the net C and N mineralized from each EOM by the total amount of added organic C and organic N by the EOM, respectively. We thus hypothesized the absence of a priming effect (Bol et al., 2003).

The EOMs were classified into 5 groups: livestock manures (n=103), composts (n=337), anaerobic digestates (n=54), sewage sludges (n=70) and others (n=99). Each EOM group was divided into different EOM subgroups (from 1 to 8). Only digestates were not subdivided into different subgroups because of the limited number of digestates in the database compared to the diversity of digestates according to process (solid or liquid state), post-treatment (phase separation or not), and digested waste (animal manures, urban wastes) and the non-significant differences in C and N mineralization among these factors.

Each EOM was described by its organic C content, its organic and mineral N contents and its C_{org}:N_{org} ratio (Table 1). For 608 of the 663 incubated EOMs, the biochemical fractions of the EOM (Van Soest & Wine, 1967) were also available. These biochemical fractions combined with the proportion of EOM organic C mineralized during 3 days of incubation in soil allowed the computation of the I_{ROC} value, which is an indicator of the proportion of the EOM organic matter remaining in soils over the long term after application (Lashermes et al., 2009) (Equation 1).

$$I_{ROC} = 44.5 + 0.5\,SOL - 0.2\,CEL + 0.7\,LIC - 2.3\,C_{3d} \quad (1)$$

where *SOL*, *CEL*, and *LIC* are the soluble, cellulose-like and lignin-like fractions (percentage of the total organic matter) and C_{3d} is the percentage of organic C mineralized during 3 days of incubation in soil (percentage of the total C)

Finally, to estimate the contributions of organic C from the EOMs to the soil organic matter and of organic N from the EOMs to the soil mineral N, the mineralized organic carbon and the mineralized organic nitrogen after a period of incubation equivalent to one year in field conditions based on mean annual temperature were computed. This equivalent incubation duration was determined by using the concept of "normalized" time (Mary et al., 1996), which modifies the incubation time with correction factors based on soil temperature and soil water content. The correction factors of the STICS model were used (Brisson et al., 2008) (see section 2.2 and Appendix A). The mean annual temperature in the field applied was 12°C, corresponding to the mean annual temperature in central France, while a constant soil water content equivalent to field capacity was used. The observed quantity of C and N mineralized were not modified, only the corresponding incubation time. For example, 89 days of incubation at 28°C and field capacity corresponded to 365 days in the field at 12°C and field capacity.

2.2 EOM decomposition model

We used a simple generic decomposition model based on the residue decomposition module of the STICS model. This model was initially developed for crop residues (Nicolardot et al., 2001). In this study, we used a modified version of the STICS decomposition module, adapted from Levavasseur et al. (2021), which allowed a better simulation of C and N mineralization from EOMs of various origins.

The soil organic matter is subdivided into five pools (Figure 1). EOM C is divided into labile (RES_1) and recalcitrant (RES_2) pools (with RES standing for "residues"). The allocation of nitrogen between these two pools can be different, with each pool having its own C:N ratio (CN_{res1} and CN_{res2}). This allocation is defined by a single parameter, a_{CN1}, which is the ratio between CN_{res1} and CN_{res}, where CN_{res} is the C:N ratio of the EOM as a whole. The labile pool decomposes according to first-order kinetics with the decomposition constant K_{res}, while the recalcitrant pool is directly incorporated into the active organic matter pool. The decomposed labile pool is either mineralized or assimilated by the zymogenous microbial biomass pool (with an assimilation yield Y). Soil mineral N may be immobilized if the C:N ratio of the labile pool (CN_{res1}) greatly exceeds that of the microbial biomass (CN_{bio}). The microbial biomass decays according to first-order kinetics, with the decomposition constant K_{bio}. The decomposed biomass is either mineralized or incorporated in the active soil organic matter, with the humification yield H. The soil mineral N may be immobilized during this decay process depending on the C:N ratio of the newly formed active soil organic matter, which is set as equal to the initial C:N ratio of the soil organic matter. The active soil organic matter decomposes according to first-order kinetics, with the decomposition constant K_a that depends on soil type (Clivot et al., 2017). In this study, however, the K_a constant was optimized to minimize the simulation error of the mineralized C and N in the control treatment, which did not include EOM in the

incubation. The stable soil organic matter pool is assumed to be inert at the century time scale. With this model, the proportion of mineralized C and N is the sum of three exponential terms (Appendix A, online supporting information).

2.3 Model calibration

Three methods of calibration (i.e., the adjustment of the model parameters) were tested. M1 included a calibration specific to each EOM, wherein the unknown decomposition parameters were optimized for each EOM separately. M2 included a calibration per EOM subgroup, assuming that all EOMs of the same subgroup had the same optimized decomposition parameters. M3 included a calibration per EOM subgroup based on measured EOM characteristics. For the M3 method, the results of the M1 calibration method were used to derive linear relationships between optimized decomposition parameters and two EOM characteristics (I_{ROC} and C_{3d}) for all the EOMs together. The parameters of these linear relationships were further optimized in calibration method M3, i.e., the decomposition parameters were predicted by using linear relationships with EOM characteristics. Simple linear functions with only I_{ROC} and C_{3d} were selected; other types of functions and other EOM characteristics available in the database (e.g., lignin content) did not significantly improve the prediction of the EOM parameters. As for the M2 method, the interest of the M3 method is to avoid the need for an additional experimental incubation for each new EOM (i.e., an EOM not in the database). In addition to M2, the objective of the M3 method is to use easily available EOM characteristics to improve the calibration within each EOM subgroup.

The upper and lower limits of the optimized parameters were mainly determined according to the literature. K_{res} varied between 0.005 and 0.7 day^{-1}. These values prevented both an accumulation of the labile pool in soil (which would not be consistent) and unrealistic decomposition in only a few days. K_{bio} was set at 0.0076 day^{-1} according to Justes et al.

(2009), assuming that the zymogenous biomass had the same decay rate for EOMs and crop residues. The assimilation yield (*Y*) varied between 0.1 and 0.6 (Lee & Schmidt, 2014; Sauvadet et al., 2018; Spohn et al., 2016). The mean value of the humification yield (*H*) optimized with calibration method M1 was 0.88. Preliminary tests indicated that fixing *H* at this value for all EOMs did not significantly decrease model performances (Table S3, Appendix B, online supporting information) due to compensation between *H*, *Y* and RES_1. This high and constant *H* value is consistent with the primary role of microbial necromass in soil organic matter formation (Miltner et al., 2012). CN_{bio} was fixed at 7, according to the mean value reported in the literature and because the C:N ratio of microbial biomass is not expected to change markedly (Mooshammer et al., 2014). Fixing CN_{bio} at this value for all EOMs did not significantly decrease model performances (Table S3, Appendix B, online supporting information). RES_1 and RES_2 varied between 0 and 1, allowing EOM to be completely labile or recalcitrant. CN_{res1} and CN_{res2} were defined as positive and to ensure the nitrogen mass balance (relative to the total amount of N in the EOMs).

For each method of model calibration, the parameters were optimized to minimize the sum of the root mean square errors (*RMSEs)* for the mineralized C and N (Equation 2).

$$RMSE = \sqrt{\frac{1}{n} \cdot \sum_{i=1}^{n} (O_i - S_i)^2} \qquad (2)$$

where S_i and O_i are the simulated and observed values for the same measurement date (*i*) and *n* is the number of measurement dates. The optimized (K_{res}) or fixed (K_{bio}) decomposition rates were corrected with the temperature and soil water content functions (Brisson et al., 2008; Mary et al., 1996) (Appendix A) to take into account the effect of these factors.

The “optim” function in R with the “L-BFGS-B” method was used for optimization (Byrd et al., 1995), giving a lower and an upper bound to each parameter, as mentioned above.

2.4 Model validation

Calibration method M1 could not be validated on an independent dataset, and the calibration was specific to each EOM. We assessed the performances of calibration methods M2 and M3 by using V-fold cross-validation with three replicates. Each EOM subgroup was randomly divided into three different subsamples. Two subsamples were used for calibration, and the third subsample was used for validation. We repeated this operation three times, changing the validation subsample each time, and then repeated these three operations three times by changing the random division of the sample to avoid any sampling effects in the results.

The performances of the model for calibration and validation were assessed with three different statistical criteria: the *RMSE*, the mean error (*ME*), and the coefficient of determination (R^2) (Equations 2, 3 and 4). These criteria were computed for each incubation and then averaged.

$$ME = \frac{1}{n} \cdot \sum_{i=1}^{n} (O_i - S_i) \quad (3)$$

$$R^2 = \left(\frac{\sum_{i=1}^{n}((O_i-\bar{O})\cdot(S_i-\bar{S}))}{\sqrt{\sum_{i=1}^{n}(O_i-\bar{O})^2}\cdot\sqrt{\sum_{i=1}^{n}(S_i-\bar{S})^2}}\right)^2 \quad (4)$$

where S_i and O_i are the simulated and observed values for the same measurement date (i) and n is the number of measurement dates. $\bar{O}$ and $\bar{S}$ are the means of the observations and simulations, respectively.

3 Results

3.1 Observed C and N mineralization

For a given EOM group, the C and N mineralization varied widely between the different EOMs (Figure 2). For example, for animal manures, the mineralized C varied between 0

and 500 mg C g^{-1} added C and the mineralized N varied between -500 and 500 mg N g^{-1} added N after twenty days of incubation. Among animal manures, chicken droppings (AM_CD) produced the greatest net mineralization, while horse manure decomposition resulted in a net N immobilization.

The calculation of mineralized C after an incubation duration equivalent to one year in the field allows an easy assessment of the potential EOM contribution to C storage in soil (the lower the mineralized C is, the higher the contribution) (Figure 3). Compared to all other EOMs, the lowest values were obtained for composts, with a median C mineralization equal to 181, 270, 372, 403 and 456 mg C g^{-1} added C for composts, digestates, animal manures, sewage sludges and other EOMs, respectively. However, a large variability was found within the EOM groups. For example, composts of municipal solid waste (C_MSW) exhibited a higher C mineralization (median value of 324 mg C g^{-1} added C) than the average, while composts of green waste (C_GW) showed a very low C mineralization, equal to 108 mg C g^{-1} added C. Differences in the mineralized C after an incubation duration equivalent to one year in the field also appeared among animal manures: chicken droppings, pig slurries and horse manures had median values of 545, 448 and 432 mg C g^{-1} added C, respectively, and were more mineralizable than bovine manure (258 mg C g^{-1} added C). If we consider all the EOM subgroups, the mineralized C after an incubation duration equivalent to one year in the field appeared to be well correlated with the I_{ROC} (R^2 = 0.67, Table S4, Appendix B, online supporting information). For specific EOM subgroups, the I_{ROC} was also significantly correlated with mineralized C, except for some EOM subgroups with low mineralization (e.g., green waste compost (C_GW), Table S4, Appendix B, online supporting information).

The calculation of net mineralized N after an incubation duration equivalent to one year in the field allowed us to compare the fertilizing values of the various EOMs (Figure 3).

Composts and digestates were characterized by a small net mineralization, which varied between -104 and 76 mg N g^{-1} added N. The short-term N fertilizing value of these EOMs thus relied on their mineral nitrogen content only, which was very low for most composts (except, e.g., C_GWS and C_PIS) but high for digestates (Table 1). Wide variability was found among the animal manures: horse manure decomposition resulted in strong N immobilization (-419 mg N g^{-1} added N), while chicken droppings produced important net N mineralization (304 mg N g^{-1} added N). Moderate amounts of N were mineralized from bovine and pig manures (52 and 100 mg N g^{-1} added N, respectively), which had small mineral N contents. The three sewage sludge subgroups exhibited a high mineralized N (278 to 432 mg N g^{-1} added N). The last group of EOMs ("others") exhibited variable N mineralization, which is consistent with the highly diverse EOMs within this group, ranging from vegetal residues (e.g., bark) that mainly immobilized N to algae and animal residues (e.g., feather meal) that mainly mineralized N. The variability in the net mineralized N after an incubation duration equivalent to one year in the field for all the EOM subgroups was partly related to that of $C{:}N_{org}$ (R^2 = 0.32, Table S4, Appendix B, online supporting information). However, the relationship between the mineralized N and $C{:}N_{org}$ varied widely among the EOM subgroups: a good correlation was observed for some EOM subgroups (e.g., R^2= 0.89 for C_PIS and R^2 = 0.92 for OTH_AR) to the absence of a relationship for other EOMs (e.g., R^2 = 0 for AM_HM and SS_AGR).

3.2 Prediction of C and N mineralization

The simulation of C and N mineralization with a calibration specific to each EOM (M1) gave very good results. The observed variability was very well accounted for (Figure 4): the determination coefficient was 0.92 for C and 0.68 for N, the bias was very low (5 mg C g^{-1} added C and 2 mg N g^{-1} added N) and the *RMSE* values were 32 mg C g^{-}

^{1} added C and 50 mg N g^{-1} added N (Table **2**), which were less than twofold the mean standard deviation of the observations (17 mg C g^{-1} added C and 39 mg N g^{-1} added N).

When using method M2, which included a calibration per EOM subgroup (i.e., all the EOMs within the same EOM subgroup had the same optimized parameters), the observed variability in C and N mineralization was still reproduced by the model (Figure 4), but the R^2 of the cross-validation for N mineralization decreased to 0.52. A slight bias was observed for C (-11 mg C g^{-1} added C), and the *RMSE* increased by a 2- to 3-fold factor for both C and N (Table **2**).

When the calibration was based on EOM characteristics (including EOM subgroup) (M3), the model performance based on the validation dataset was better than the performance observed for method M2, since the *RMSE* of mineralized C dropped from 99 to 65 mg C g^{-1} added C and the *RMSE* of mineralized N decreased from 126 to 110 mg N g^{-1} added N.

Regardless of the calibration method, the model performance strongly varied with EOM subgroup (Tables S3 and S4, Appendix B, online supporting information). For example, the highest *RMSE* was often associated with the EOM that had the highest mineralization (e.g. algae (OTH_ALG) and agri-industrial wastewater (OTH_AGRWW)).

3.3 Parameters of the calibration per EOM subgroup

For calibration method M2, a set of parameters was proposed for each EOM subgroup (Table 3). In the absence of a specific incubation for a given EOM or of its characteristics (e.g., I_{ROC}), these parameters can be used to simulate C and N mineralization with acceptable accuracy (section 3.2). The parameters greatly varied according to EOM subgroup. The labile fraction of the residues (RES_1) varied between 0.13 for the green waste compost (C_GW) and 1.00 for vinasse (OTH_VIN) and algae (OTH_ALG). The microbial assimilation yield (Y) ranged from 0.10 (for example, in chicken droppings

(AM_CD)) to 0.60 in green waste and sludge compost (C_GWS). The parameter aCN_1 was greater than 1 for all EOMs except SS_AGR, indicating that the C:N ratio of the labile pool (CN_{res1}) was greater than the C:N ratio of the recalcitrant pool (CN_{res2}). The corresponding simulated C and N mineralization dynamics for the different EOM subgroups are presented in Figure S1 (Appendix C, online supporting information).

3.4 Parameters of the calibration per EOM subgroup and with EOM characteristics

For calibration method M3, the relationships between the model parameters and EOM characteristics were established by considering the significant relationships observed between the optimized parameters of EOM in the first calibration method (M1) and EOM characteristics (Figure S2). The labile fractions of the EOMs (RES_1) decreased with increasing values of I_{ROC} (R^2=0.61 with EOM subgroup as a covariable, R^2 = 0.49 for all the EOMs together). The decomposition rate (K_{res}) increased with C_{3d} according to a logarithmic relationship (R^2 = 0.34 with EOM subgroup as a covariable, R^2 = 0.21 for all the EOMs together). The other significant relationships were not considered because they did not improve the residual variance. The aforementioned linear relationships were introduced in calibration method M3 to predict the EOM parameters of the model (Table 4 and Table S7, Appendix B, online supporting information). EOM subgroup was added as a covariable due to the systematic improvement in R^2 when using it.

4 Discussion

4.1 Variability in EOM C and N mineralization

The comparison of a wide range of EOMs highlighted some important differences in C and N mineralization among the EOMs (Figure 2, Figure 3). While C mineralization from the EOMs was generally low for composts, C mineralization can be high for certain EOMs, such as chicken droppings, animal residues or vinasses. The rate of N mineralization from

the EOMs exhibited even more variability between EOM subgroups (e.g., important net N mineralization for chicken droppings and strong net N immobilization for horse manure). Considering the organic N content of these two EOMs (Table 1), their typical water content (60% and 30%, respectively, personal data) and their typical application rate (20 and 3 t ha^{-1}, respectively, personal data), the input of organic N would represent approximately 100 kg ha^{-1} in both cases, thus leading to a net immobilization of 42 kg N ha^{-1} for horse manure and a net mineralization of 30 kg N ha^{-1} for chicken droppings after one year in the field. Despite the high immobilization caused by horse manure in the first phase, this EOM could have a fertilizing value during the second phase, in which N is slowly released (Figure 2). Moreover, it is important to highlight that these high values of N immobilization represents only the potential immobilization, which can be reached only when the soil mineral N content is large enough and is a nonlimiting factor in decomposition. The hierarchy of amendment and fertilizing values between the EOM subgroups is in line with existing literature (Lazicki et al., 2020; Mondini et al., 2017; Noirot-Cosson et al., 2017), even though the comparison of so many EOM subgroups is rare. The hierarchy of mineralized C and N after an incubation duration equivalent to one year in the field between the EOM subgroups also reflected their contribution to the SOC (inverse relationship) observed in the field by various authors (Gerzabek et al., 1997; Levavasseur et al., 2020) and to N short-term supply (Gutser et al., 2005).

In addition to the differences between EOM subgroups, a high variability in C and N mineralization existed inside each EOM subgroup (Figure 3). This result highlighted the need for a detailed characterization of EOMs, either through laboratory incubations, or with indicators that are easier to retrieve, such as the I_{ROC} indicator based on biochemical fractionation (Lashermes et al., 2009), to determine the contribution of EOMs to SOC. We found a strong correlation between the mineralized C after an incubation duration

equivalent to one year in the field and I_{ROC} (R^2 = 0.67), which was expected because I_{ROC} was defined as a predictor of residual C in soils under laboratory incubation. Our study, however, validates the interest of I_{ROC} for a wider range of EOMs, including for some EOM subgroups not used in the I_{ROC} calibration such as digestates (R^2 between mineralized C and I_{ROC} equal to 0.62). The mineralized N after an incubation duration equivalent to one year in the field was less but significantly correlated with EOM characteristics (R^2 with CN_{res} equal to 0.32), and the correlation was higher for some EOM subgroups (e.g., animal residues (OTH_AR)). This result contradicts a study showing that CN_{res} was a good predictor of N mineralization (R^2 = 0.94) (Lazicki et al., 2020) but confirms another study pointing out that CN_{res} is not sufficient for predicting the N mineralization of EOMs of various qualities (Bonanomi et al., 2019). The limited capacity of this parameter to predict N mineralization could be explained by the great diversity of EOMs used in our study. For example, some anaerobic digestates exhibited low CN_{res} and induced N immobilization, in opposition to other EOM with low CN_{res} like sewage sludge. Moreover, the use of incubations realized in different experimental conditions in our study (temperature, water content) and their "standardization" using the concept of normalized time (Mary et al., 1996) could partly weaken the relationship between EOM characteristics and EOM mineralization for all the incubation taken together, even if most of the EOM incubation that we used were realized in similar conditions (Tables S1 and S2).

Despite the interest in EOM characteristics, they were not sufficient to predict the dynamics of C and N mineralization in various soil and climate conditions, which required the use of a well-calibrated decomposition model.

4.2 Model performance

The calibration of individual EOMs in the model yielded good model performances for all the EOM subgroups, with *RMSE* values equal to 32 mg C g^{-1} added C and 50 mg N g^{-}

[1] added N and an R^2 equal to 0.92 and 0.68 for C and N mineralization, respectively. These performances are similar to those reported for other models for a less diverse groups of EOMs (Gale et al., 2006; Mohanty et al., 2011; Mondini et al., 2017). It is also comparable to the performance obtained with the STICS model for crop residues (Justes et al., 2009). When the same set of parameters was used for all the EOMs of the same EOM subgroup, the model performances decreased for C and N, due to the diversity of EOMs within each subgroup. The simulation of C mineralization was improved when the EOM characteristics (I_{ROC} and C_{3ds}) were accounted for in the model parameterization. However, the EOM characteristics were not sufficient for the determination of decomposition parameters capable of simulating the N mineralization kinetics very accurately. Such a result was found by Noirot-Cosson et al. (2017) and Monhanty et al. (2011).

Regarding the model performances within the three calibration methods, we recommend that a specific EOM laboratory incubation is used to calibrate the model (M1 method) and to most accurately predict its potential behavior in the field, when the user considers a specific EOM (Figure 5). However, model users often do not have any information on the particular EOM, except the quantity applied. In that case, we showed that a calibration depending only on its subgroup (M2 method) bring some insights that are sufficient to test some global EOM application scenarios. We do not recommend to use the M2 “default” method to simulate accurately the effects of a specific EOM in case of repeated application so as not to accumulate over time the error in the estimates. As an alternative to the latter case, we highly recommend the addition of EOM easily measurable characteristics to calibrate the model (M3 method), as tested in Levavasseur et al. (2021) for the simulation of a long term experiment. The quality of the calibration methods M2 and M3 varied according to the considered EOM subgroup (Table S5 and S6). We recommend the user to consider the EOM subgroup to determine whether a specific calibration of the modeled

EOM (M1) is required or not and to put it in perspective with the objective and characteristics of the modeling study (e.g., importance of EOM application in the scenarios).

Other EOM characteristics not considered here might contribute to improving the prediction of EOM model parameters and, subsequently, the simulation of C and N mineralization. For example, the C:N ratio of biochemical fractions has been shown to be useful in predicting N mineralization (Morvan & Nicolardot, 2009; Parnaudeau et al., 2004) as well as 13C-CPMAS NMR spectral regions (Bonanomi et al., 2019; Pansu et al., 2017). However, these characteristics were not available in the EOM database we used and are not usually available outside research laboratories. The identification of readily available EOM characteristics that can be used to calibrate decomposition models remains a challenge.

4.3 Model hypotheses

The modification of the STICS model proposed by Levavasseur et al. (2021) to model EOM decomposition was used to simulate a wide range of EOM decomposition levels in our study. This modification includes the addition of a recalcitrant pool of EOM that is directly incorporated in the soil active OM and is not assimilated by the microbial biomass, assuming that this recalcitrant pool results from the previous digestion of raw matter by microbial biomass (in animal guts or during treatments). This pool is considered to have the same dynamics as the active pool in the STICS model. Several authors have hypothesized that EOM is composed of at least two dynamic pools (Gijsman et al., 2002; Mondini et al., 2017) to simulate EOM decomposition; however, this distinction was not necessary for simulating crop residue decomposition in the STICS model, which considered a single dynamic pool (Justes et al., 2009). Whereas the decay rate of the recalcitrant pool of EOM was optimized and inferior to the decay rate of the soil active

433 OM in the study of Levavasseur et al. (2021), this decay rate was set equal to that of the
434 soil active OM in the present study. This simplification caused some overestimation of C
435 mineralization for very stable EOMs, such as composts (Figure 4). The plateau of C
436 mineralization usually observed in laboratory incubations could not be properly simulated
437 with this model. However, this modification was made to limit the number of parameters in
438 the STICS model. Moreover, several authors have suggested that SOM stability after EOM
439 application is not modified (Liu et al., 2018; Luan et al., 2019), even though another study
440 suggested the opposite (Peltre et al., 2017). Levavasseur et al. (2020) successfully
441 simulated carbon storage in long-term field experiments with EOM application using the
442 AMG model without assuming a greater stability of EOM in comparison to that of SOM.
443 Because the STICS and AMG formalisms for SOC are very similar (i.e., SOC is divided
444 into an active and a stable pool, and the mineralization function is the same) (Clivot et al.,
445 2019), the STICS model should also allow the simulation of C and N dynamics of EOMs
446 without assuming a greater stability of those EOMs, i.e., by allocating EOMs only to soil
447 active OM (either directly, or after soil microbial biomass assimilation, Figure 1). Directly
448 allocating the recalcitrant fractions of EOMs to soil active OM could change the soil C:N
449 ratio after repeated applications of the EOMs. This effect is consistent with the fact that
450 soil C:N usually increases with SOC content (Mooshammer et al., 2014). Other
451 simplifications made in our study include the use of a constant humification yield (H) of
452 microbial necromass and a constant C:N ratio of microbial biomass (CN_{bio}), in line with
453 recent knowledge about SOM formation (Miltner et al., 2012; Mooshammer et al., 2014).
454 However, the H value retained in our study is higher than the value reported in the study of
455 Miltner et al. (2012). Concerning the decay rate of the labile pool K_{res}, the calibration
456 method M1 gave some optimized values equal to the minimal (0.005 day^{-1}) or maximal
457 (0.7 day^{-1}) value for some EOM (Figure S2). The use of lower minimal and higher

maximal values could improve the simulation. However, we decided to keep these limits to prevent both an accumulation of the labile pool in soil (which would not be consistent) and unrealistic decomposition in only a few days.

The use of EOM incubations to calibrate the decomposition module of the STICS model and predict EOM decomposition under field conditions requires some correction factors regarding water content and temperature. The use of EOM incubations run under different conditions (temperature, soil water content, soil type) could have introduced errors into the EOM calibration, because of the uncertainty associated with these correction factors. However, most of the EOM incubations used in this study were realized in similar conditions (loamy soil, 28°C, water content close to or equal to field capacity, Tables S1 and S2). The effects of soil type, water content, temperature and N mineral availability are already taken into account in the STICS soil-crop model to calculate EOM mineralization *in situ* (Brisson et al., 2008). The correction factors should allow the extrapolation of laboratory incubations to field conditions (Gale et al., 2006). However, laboratory incubations are usually realized with dried and crushed EOM, which can influence the mineralization of C and, especially, N (Le Roux et al., 2016). Correction factors that consider EOM preparation before incubation should also be proposed.

Finally, beyond the STICS users, the decomposition module (Appendix A) and the calibrations proposed in this paper could be used outside the STICS model to predict the C and N mineralization of a large diversity of EOMs.

5 Conclusions

We quantified the C and N mineralization of a wide range of EOMs based on a database of more than 600 EOM incubations, from five groups (animal manures, composts, sewage sludges, digestates, and others) and 26 subgroups (e.g., bovine manure, green waste

compost). This represents one of the largest and most diversified syntheses of EOM incubation data. The results indicated a wide diversity in EOM contributions to C storage in soil and N supply for crops, both between EOM subgroups and within EOMs of the same subgroup. The EOM incubations were used to calibrate a simple generic decomposition model included in the STICS soil-crop model to simulate EOM decomposition. Individual EOM calibration yielded the best model performances for the simulation of C and N mineralization and is the recommended calibration method of the STICS model for accurate simulations of scenarios of application of a specific EOM in field conditions. In the absence of EOM incubation data, we proposed two calibration methods for the 26 different subgroups of EOMs in the STICS model: using either a unique calibration per EOM subgroup or EOM characteristics as predictors of model parameters. Although these two calibration methods decreased model performances, they allow the prediction with a reasonable performance of the EOM contribution to soil C storage or to mineral N supply to determine the best practices for their use (amount, period of application, fertilized crops, etc.). Future research is needed to better predict the EOM parameters from easily available EOM characteristics and verify the extrapolation of laboratory incubation to field conditions.

6 Acknowledgements

We are grateful to the companies LDAR, Auréa, Rittmo and Frayssinet for providing some of the EOM incubation data.

7 References

AFNOR. (2009). Norme XP U 44-163. Amendements organiques et supports de culture—Caractérisation de la matière organique par la minéralisation potentielle du carbone et de l'azote.

Bol, R., Moering, J., Kuzyakov, Y., & Amelung, W. (2003). Quantification of priming and CO2 respiration sources following slurry-C incorporation into two grassland soils with different C content. Rapid Communications in Mass Spectrometry, 17(23), 2585–2590. https://doi.org/10.1002/rcm.1184

Bonanomi, G., Sarker, T. C., Zotti, M., Cesarano, G., Allevato, E., & Mazzoleni, S. (2019). Predicting nitrogen mineralization from organic amendments: Beyond C/N ratio by 13C-CPMAS NMR approach. Plant and Soil, 441(1), 129–146. https://doi.org/10.1007/s11104-019-04099-6

Brisson, N., Launay, M., Mary, B., & Beaudoin, N. (2008). Conceptual Basis, Formalisations and Parameterization of the STICS Crop Model (Editions Quae).

Byrd, R., Lu, P., Nocedal, J., & Zhu, C. (1995). A Limited Memory Algorithm for Bound Constrained Optimization. SIAM Journal on Scientific Computing, 16(5), 1190–1208. https://doi.org/10.1137/0916069

Chenu, C., Angers, D. A., Barré, P., Derrien, D., Arrouays, D., & Balesdent, J. (2019). Increasing organic stocks in agricultural soils: Knowledge gaps and potential innovations. Soil and Tillage Research, 188, 41–52. https://doi.org/10.1016/j.still.2018.04.011

Clivot, H., Mary, B., Valé, M., Cohan, J.-P., Champolivier, L., Piraux, F., Laurent, F., & Justes, E. (2017). Quantifying in situ and modeling net nitrogen mineralization from soil organic matter in arable cropping systems. Soil Biology and Biochemistry, 111, 44–59. https://doi.org/10.1016/j.soilbio.2017.03.010

528 Clivot, H., Mouny, J.-C., Duparque, A., Dinh, J.-L., Denoroy, P., Houot, S., Vertès, F.,
529 Trochard, R., Bouthier, A., Sagot, S., & Mary, B. (2019). Modeling soil organic
530 carbon evolution in long-term arable experiments with AMG model. Environmental
531 Modelling & Software, 118, 99–113. https://doi.org/10.1016/j.envsoft.2019.04.004
532 Delin, S., Stenberg, B., Nyberg, A., & Brohede, L. (2012). Potential methods for
533 estimating nitrogen fertilizer value of organic residues. Soil Use and Management,
534 28(3), 283–291. https://doi.org/10.1111/j.1475-2743.2012.00417.x
535 Gale, E. S., Sullivan, D. M., Cogger, C. G., Bary, A. I., Hemphill, D. D., & Myhre, E. A.
536 (2006). Estimating Plant-Available Nitrogen Release from Manures, Composts, and
537 Specialty Products. Journal of Environmental Quality, 35(6), 2321–2332.
538 https://doi.org/10.2134/jeq2006.0062
539 Gerzabek, M. h., Pichlmayer, F., Kirchmann, H., & Haberhauer, G. (1997). The response
540 of soil organic matter to manure amendments in a long-term experiment at Ultuna,
541 Sweden. European Journal of Soil Science, 48(2), 273–282.
542 https://doi.org/10.1111/j.1365-2389.1997.tb00547.x
543 Gijsman, A. J., Hoogenboom, G., Parton, W. J., & Kerridge, P. C. (2002). Modifying
544 DSSAT Crop Models for Low-Input Agricultural Systems Using a Soil Organic
545 Matter–Residue Module from CENTURY. Agronomy Journal, 94(3), 462–474.
546 https://doi.org/10.2134/agronj2002.4620
547 Gómez-Muñoz, B., Magid, J., & Jensen, L. S. (2017). Nitrogen turnover, crop use
548 efficiency and soil fertility in a long-term field experiment amended with different
549 qualities of urban and agricultural waste. Agriculture, Ecosystems & Environment,
550 240, 300–313. https://doi.org/10.1016/j.agee.2017.01.030
551 Gutser, R., Ebertseder, Th., Weber, A., Schraml, M., & Schmidhalter, U. (2005). Short-
552 term and residual availability of nitrogen after long-term application of organic

fertilizers on arable land. Journal of Plant Nutrition and Soil Science, 168(4), 439–446. https://doi.org/10.1002/jpln.200520510

Justes, E., Mary, B., & Nicolardot, B. (2009). Quantifying and modelling C and N mineralization kinetics of catch crop residues in soil: Parameterization of the residue decomposition module of STICS model for mature and non mature residues. Plant and Soil, 325(1–2), 171–185. https://doi.org/10.1007/s11104-009-9966-4

Lashermes, G., Nicolardot, B., Parnaudeau, V., Thuriès, L., Chaussod, R., Guillotin, M. L., Linères, M., Mary, B., Metzger, L., Morvan, T., Tricaud, A., Villette, C., & Houot, S. (2009). Indicator of potential residual carbon in soils after exogenous organic matter application. European Journal of Soil Science, 60(2), 297–310. https://doi.org/10.1111/j.1365-2389.2008.01110.x

Lashermes, G., Nicolardot, B., Parnaudeau, V., Thuriès, L., Chaussod, R., Guillotin, M. L., Linères, M., Mary, B., Metzger, L., Morvan, T., Tricaud, A., Villette, C., & Houot, S. (2010). Typology of exogenous organic matters based on chemical and biochemical composition to predict potential nitrogen mineralization. Bioresource Technology, 101(1), 157–164. https://doi.org/10.1016/j.biortech.2009.08.025

Lazicki, P., Geisseler, D., & Lloyd, M. (2020). Nitrogen mineralization from organic amendments is variable but predictable. Journal of Environmental Quality, 49(2), 483–495. https://doi.org/10.1002/jeq2.20030

Le Roux, C., Damay, N., Servain, F., Machet, J. M., Houot, S., & Recous, S. (2016, June 27). Effects of crushing and drying organic products on their nitrogen and carbon mineralization in soil incubations. 19 th Nitrogen Workshop - Efficient use of different sources of Nitrogen in agriculture – from theory to practice, Skara, Sweden.

578 Lee, Z. M., & Schmidt, T. M. (2014). Bacterial growth efficiency varies in soils under
579 different land management practices. Soil Biology and Biochemistry, 69, 282–290.
580 https://doi.org/10.1016/j.soilbio.2013.11.012
581 Levavasseur, F., Mary, B., Christensen, B. T., Duparque, A., Ferchaud, F., Kätterer, T.,
582 Lagrange, H., Montenach, D., Resseguier, C., & Houot, S. (2020). The simple
583 AMG model accurately simulates organic carbon storage in soils after repeated
584 application of exogenous organic matter. Nutrient Cycling in Agroecosystems.
585 https://doi.org/10.1007/s10705-020-10065-x
586 Levavasseur, F., Mary, B., & Houot, S. (2021). C and N dynamics with repeated organic
587 amendments can be simulated with the STICS model. Nutrient Cycling in
588 Agroecosystems. https://doi.org/10.1007/s10705-020-10106-5
589 Liu, H., Zhang, J., Ai, Z., Wu, Y., Xu, H., Li, Q., Xue, S., & Liu, G. (2018). 16-Year
590 fertilization changes the dynamics of soil oxidizable organic carbon fractions and
591 the stability of soil organic carbon in soybean-corn agroecosystem. Agriculture,
592 Ecosystems & Environment, 265, 320–330.
593 https://doi.org/10.1016/j.agee.2018.06.032
594 Luan, H., Gao, W., Huang, S., Tang, J., Li, M., Zhang, H., & Chen, X. (2019). Partial
595 substitution of chemical fertilizer with organic amendments affects soil organic
596 carbon composition and stability in a greenhouse vegetable production system. Soil
597 and Tillage Research, 191, 185–196. https://doi.org/10.1016/j.still.2019.04.009
598 Mary, B., Recous, S., Darwis, D., & Robin, D. (1996). Interactions between decomposition
599 of plant residues and nitrogen cycling in soil. Plant and Soil, 181(1), 71–82.
600 https://doi.org/10.1007/BF00011294

601 Miltner, A., Bombach, P., Schmidt-Brücken, B., & Kästner, M. (2012). SOM genesis:
602 Microbial biomass as a significant source. Biogeochemistry, 111(1), 41–55.
603 https://doi.org/10.1007/s10533-011-9658-z
604 Mohanty, M., Reddy, K. S., Probert, M. E., Dalal, R. C., Rao, A. S., & Menzies, N. W.
605 (2011). Modelling N mineralization from green manure and farmyard manure from
606 a laboratory incubation study. Ecological Modelling, 222(3), 719–726.
607 https://doi.org/10.1016/j.ecolmodel.2010.10.027
608 Mondini, C., Cayuela, M. L., Sinicco, T., Fornasier, F., Galvez, A., & Sánchez-Monedero,
609 M. A. (2017). Modification of the RothC model to simulate soil C mineralization of
610 exogenous organic matter. Biogeosciences, 14(13), 3253–3274.
611 https://doi.org/10.5194/bg-14-3253-2017
612 Mooshammer, M., Wanek, W., Zechmeister-Boltenstern, S., & Richter, A. A. (2014).
613 Stoichiometric imbalances between terrestrial decomposer communities and their
614 resources: Mechanisms and implications of microbial adaptations to their resources.
615 Frontiers in Microbiology, 5. https://doi.org/10.3389/fmicb.2014.00022
616 Morvan, T., & Nicolardot, B. (2009). Role of organic fractions on C decomposition and N
617 mineralization of animal wastes in soil. Biology and Fertility of Soils, 45(5), 477–
618 486. https://doi.org/10.1007/s00374-009-0355-1
619 Nicolardot, B., Recous, S., & Mary, B. (2001). Simulation of C and N mineralisation
620 during crop residue decomposition: A simple dynamic model based on the C:N
621 ratio of the residues. Plant and Soil, 228(1), 83–103.
622 https://doi.org/10.1023/A:1004813801728
623 Noirot-Cosson, P. E., Dhaouadi, K., Etievant, V., Vaudour, E., & Houot, S. (2017).
624 Parameterisation of the NCSOIL model to simulate C and N short-term

mineralisation of exogenous organic matter in different soils. Soil Biology and Biochemistry, 104, 128–140. https://doi.org/10.1016/j.soilbio.2016.10.015

Noirot-Cosson, P. E., Vaudour, E., Gilliot, J. M., Gabrielle, B., & Houot, S. (2016). Modelling the long-term effect of urban waste compost applications on carbon and nitrogen dynamics in temperate cropland. Soil Biology and Biochemistry, 94, 138–153. https://doi.org/10.1016/j.soilbio.2015.11.014

Pansu, M., & Thuriès, L. (2003). Kinetics of C and N mineralization, N immobilization and N volatilization of organic inputs in soil. Soil Biology and Biochemistry, 35(1), 37–48. https://doi.org/10.1016/S0038-0717(02)00234-1

Pansu, M., Thuriès, L. J.-M., Soares, V. F., Simões, M. L., & Neto, L. M. (2017). Modelling the transformation of organic materials in soil with nuclear magnetic resonance spectra. European Journal of Soil Science, 68(1), 90–104. https://doi.org/10.1111/ejss.12405

Parnaudeau, V., Nicolardot, B., & Pagès, J. (2004). Relevance of Organic Matter Fractions as Predictors of Wastewater Sludge Mineralization in Soil. Journal of Environmental Quality, 33(5), 1885–1894. https://doi.org/10.2134/jeq2004.1885

Peltre, C., Gregorich, E. G., Bruun, S., Jensen, L. S., & Magid, J. (2017). Repeated application of organic waste affects soil organic matter composition: Evidence from thermal analysis, FTIR-PAS, amino sugars and lignin biomarkers. Soil Biology and Biochemistry, 104, 117–127. https://doi.org/10.1016/j.soilbio.2016.10.016

Pinto, R., Brito, L. M., & Coutinho, J. (2020). Nitrogen Mineralization from Organic Amendments Predicted by Laboratory and Field Incubations. Communications in Soil Science and Plant Analysis, 51(4), 515–526. https://doi.org/10.1080/00103624.2020.1717510

649 Recous, S., Robin, D., Darwis, D., & Mary, B. (1995). Soil inorganic N availability: Effect
650 on maize residue decomposition. Soil Biology and Biochemistry, 27(12), 1529–
651 1538. https://doi.org/10.1016/0038-0717(95)00096-W
652 Sauvadet, M., Lashermes, G., Alavoine, G., Recous, S., Chauvat, M., Maron, P.-A., &
653 Bertrand, I. (2018). High carbon use efficiency and low priming effect promote soil
654 C stabilization under reduced tillage. Soil Biology and Biochemistry, 123, 64–73.
655 https://doi.org/10.1016/j.soilbio.2018.04.026
656 Spohn, M., Klaus, K., Wanek, W., & Richter, A. (2016). Microbial carbon use efficiency
657 and biomass turnover times depending on soil depth – Implications for carbon
658 cycling. Soil Biology and Biochemistry, 96, 74–81.
659 https://doi.org/10.1016/j.soilbio.2016.01.016
660 Van Soest, P. J., & Wine, R. H. (1967). Use of detergents in the analysis of fibrous feeds.
661 IV. Determination of plant cell-wall constituents. Journal of the Association of
662 Official Analytical Chemists, 50, 50–55.
663
664

8 Tables

667 **Table 1** Main characteristics of the EOM database

Group	Subgroup	Code	No. of samples	C_{org} (g kg^{-1} DM)		N_{org} (g kg^{-1} DM)		C_{org}:N_{org}		N_{min} (g kg^{-1} DM)		I_{ROC}* (%)	
				Mean	SD	Mean	SD	Mean	SD	Mean	SD	Mean	SD
Animal manures	Bovine manure	AM_BM	45	359	69	21.1	5.2	18.1	6.5	1.3	1.4	59	13
	Bovine slurry	AM_BS	3	360	25	33.7	11.2	12.0	5.2	25.6	11.3	51	6
	Chicken droppings	AM_CD	8	398	147	45.2	17.4	9.6	3.8	2.9	2.2	27	21
	Horse manure	AM_HM	8	407	41	12.4	2.4	33.6	5.5	0.5	0.5	50	5
	Other manures	AM_OTH	8	366	75	32.9	12.8	12.9	5.2	24.8	40.0	58	8
	Pig manure	AM_PIM	6	428	29	18.1	3.9	24.9	6.9	2.4	1.8	57	12
	Pig slurry	AM_PIS	10	409	106	37.8	17.1	11.9	3.6	30.7	30.2	47	10
	Poultry manure	AM_POM	15	353	66	26.1	8.5	14.2	3.0	4.0	4.6	47	19
Composts	Composted animal manure	C_AM	39	322	81	22.0	6.8	14.9	5.4	1.4	1.8	67	14
	Biowaste and green waste compost	C_BIO	52	212	61	16.3	4.5	13.1	2.4	0.4	0.6	75	9
	Green waste compost	C_GW	25	247	57	15.7	5.3	18.2	11.0	0.3	1.3	80	7
	Green waste and animal manure compost	C_GW+AM	9	213	98	17.6	8.7	12.4	2.1	2.1	2.1	62	12
	Green waste and sludge compost	C_GWS	71	257	64	20.0	5.2	13.6	4.8	2.2	1.8	79	10
	Municipal solid waste compost	C_MSW	89	253	72	13.1	4.1	20.1	5.8	0.8	1.0	55	15
	Other composts	C_OTH	41	299	112	17.5	8.7	23.4	22.6	1.0	1.5	69	15
	Pig slurry compost (various cosubstrates)	C_PIS	11	338	66	22.0	10.3	18.9	10.0	3.9	4.3	64	13
Digestates	All digestates	DIG	54	346	90	26.6	15.1	15.9	7.1	36.4	66.3	66	13
Sewage sludges	Agro-industrial sludges	SS_AGR	11	235	143	28.6	24.4	24.5	33.8	3.3	6.2	52	15
	Other sludges	SS_OTH	6	341	42	41.4	18.0	10.5	7.2	2.4	2.0	61	3
	Urban sludges	SS_URB	53	294	86	39.4	17.5	8.9	7.1	4.4	6.1	49	17
Others	Agro-industrial wastewater	OTH_AGRWW	23	312	158	8.7	0.7	23.4	19.1	10.0	8.3	-	-
	Algae	OTH_ALG	5	155	51	13.0	4.3	12.4	1.9	0.1	0.0	21	22
	Animal residues (feather meal, etc.)	OTH_AR	6	476	61	103.4	59.5	7.7	6.7	5.9	7.0	51	23
	Others	OTH_OTH	38	293	132	37.0	37.2	13.8	10.9	3.6	8.5	46	23
	Sugarbeet vinasse	OTH_VIN	8	352	26	34.0	7.9	11.9	2.9	1.2	0.7	-	-
	Vegetal residues (bark, grape marc, etc.)	OTH_VR	19	483	47	22.7	17.7	38.5	31.4	0.5	1.4	63	16

668 * Indicator of residual organic carbon in soils (Lashermes et al., 2009)

669 **Table 2** Model performance per incubation for all the EOMs together according to the
670 calibration method (mean calibration and validation performance of the cross-validation
671 iterations for methods M2 and M3) (ME: mean error, RMSE: root mean square error, R^2:
672 coefficient of determination).

		Carbon mineralization (mg C g^{-1} added C)			Nitrogen mineralization (mg N g^{-1} added N)		
Calibration method	Evaluation dataset	ME	RMSE	R^2	ME	RMSE	R^2
M1: Individual EOM calibration	Calibration	5	32	0.92	2	50	0.68
M2: Calibration per EOM subgroup	Calibration	-12	91	0.91	6	111	0.54
	Validation	-11	99	0.91	4	126	0.52
M3: Calibration with EOM characteristics	Calibration	-7	58	0.92	11	96	0.54
	Validation	-7	65	0.92	11	110	0.52

673

674

675 **Table 3** Optimized parameters for the STICS decomposition module per EOM subgroup
676 (obtained with the whole EOM dataset used for calibration method M2). K_{bio}, H and CN_{bio}
677 were fixed at 0.0076 day^{-1}, 0.88 and 7.0, respectively. The meaning of the EOM subgroup can
678 be found in Table 1.

EOM subgroup	K_{res} (day^{-1})	RES_1	Y	a_{CN1}
AM_BM	0.025	0.24	0.32	3.09
AM_BS	0.062	0.42	0.39	2.14
AM_CD	0.077	0.46	0.10	1.37
AM_HM	0.028	0.48	0.31	10.00
AM_OTH	0.005	1.00	0.53	1.02
AM_PIM	0.011	0.25	0.35	1.14
AM_PIS	0.048	0.40	0.10	5.25
AM_POM	0.055	0.46	0.34	1.99
C_AM	0.005	0.33	0.44	2.07
C_BIO	0.005	0.16	0.50	10.00
C_GW	0.005	0.13	0.60	10.00
C_GW+AM	0.026	0.29	0.56	10.00
C_GWS	0.005	0.18	0.60	5.58
C_MSW	0.059	0.44	0.50	1.65
C_OTH	0.005	0.19	0.58	4.29
C_PIS	0.036	0.34	0.57	1.04
DIG	0.024	0.24	0.25	10.00
SS_AGR	0.090	0.29	0.20	0.76
SS_OTH	0.076	0.48	0.52	1.04
SS_URB	0.072	0.53	0.40	1.21
OTH_AGRWW	0.141	0.64	0.38	1.71
OTH_ALG	0.069	1.00	0.25	2.38
OTH_AR	0.068	0.77	0.45	1.27
OTH_OTH	0.069	0.45	0.33	1.45
OTH_VIN	0.114	1.00	0.45	1.12
OTH_VR	0.013	0.35	0.39	10.00

679

680

681 **Table 4** Calibration for the STICS model per EOM subgroup and according to the EOM
682 characteristics (M3) (the numerical values of α_{res1}, β_{res1}, α_{kres}, β_{kres}, Y, a_{CN1} per EOM subgroup
683 are given in Table S7)

Parameter	Calibration per EOM subgroup
RES_1	$\alpha_{res1} + \beta_{res1} \times I_{ROC}$
RES_2	$1 - RES_2$
K_{res}	$\exp(\alpha_{kres} + \beta_{kres} \times C_{3d})$
K_{bio}	0.0076
Y	Y
H	0.88
CN_{bio}	7.0
a_{CN1}	a_{CN1}

684

685

9 Figure legends

Figure 1 Decomposition model of EOM in the modified version of the STICS model. The C fluxes are represented as solid black lines, and the N fluxes are represented as dashed gray lines.

RES_1 and RES_2 are the proportions of C from the EOMs in the labile pool and recalcitrant pools, respectively, with $RES_2 = 1 - RES_1$

CN_{res}, CN_{res1} and CN_{res2} are the C:N ratios of the EOM and the labile and recalcitrant pools, respectively, and a_{CN1} is the ratio $CN_{res1} : CN_{res}$

K_{res1} is the decomposition rate of the labile pool

Y is the C assimilation yield of the labile pool

CN_{bio}, CN_a and CN_s are the C:N ratios of the microbial biomass, and active and stable pools, respectively

K_{bio} and K_a are the decay rates of the zymogenous biomass and the active soil organic matter pools, respectively

H is the C humification yield.

Figure 2 Observed mineralized organic carbon and nitrogen for the different groups of EOMs in laboratory incubations. Each gray line represents an EOM incubation, while the colored lines represent fitted local polynomial regressions per EOM subgroup (performed with the loess function in R). Very few data on N mineralization are lower than -100% and the Y-axis was cut to -100% to improve the visibility. The meaning of the EOM subgroup abbreviations can be found in Table 1.

Figure 3 Observed mineralized carbon and net mineralized nitrogen for each EOM group and subgroup after incubation for a duration equivalent to one year under field conditions. The meaning of the EOM subgroup abbreviations can be found in Table 1.

Figure 4 Observed and simulated values of carbon and nitrogen mineralization for each EOM and sampling date, according to the calibration method (results obtained by using the whole EOM dataset for calibration).

Figure 5. Conceptual diagram for the calibration of an EOM in the decomposition model.

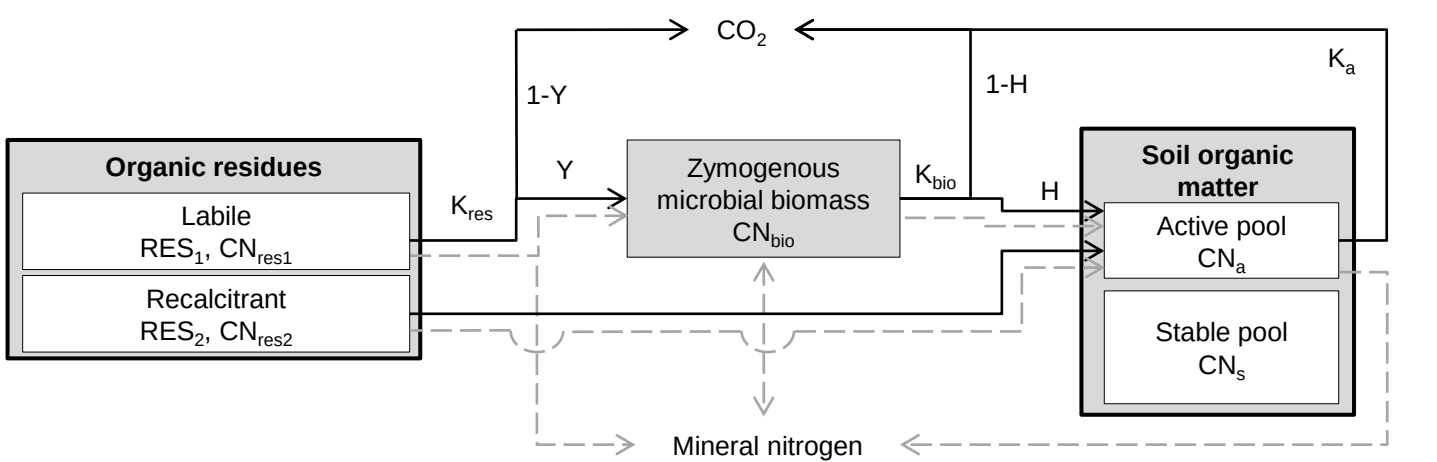
CO2
1-Y
1-H
Ka
Organic residues
Labile
RES1, CNres1
Recalcitrant
RES2, CNres2
Kres
Y
Zymogenous
microbial biomass
CNbio
Kbio
H
Soil organic
matter
Active pool
CNa
Stable pool
CNs
Mineral nitrogen

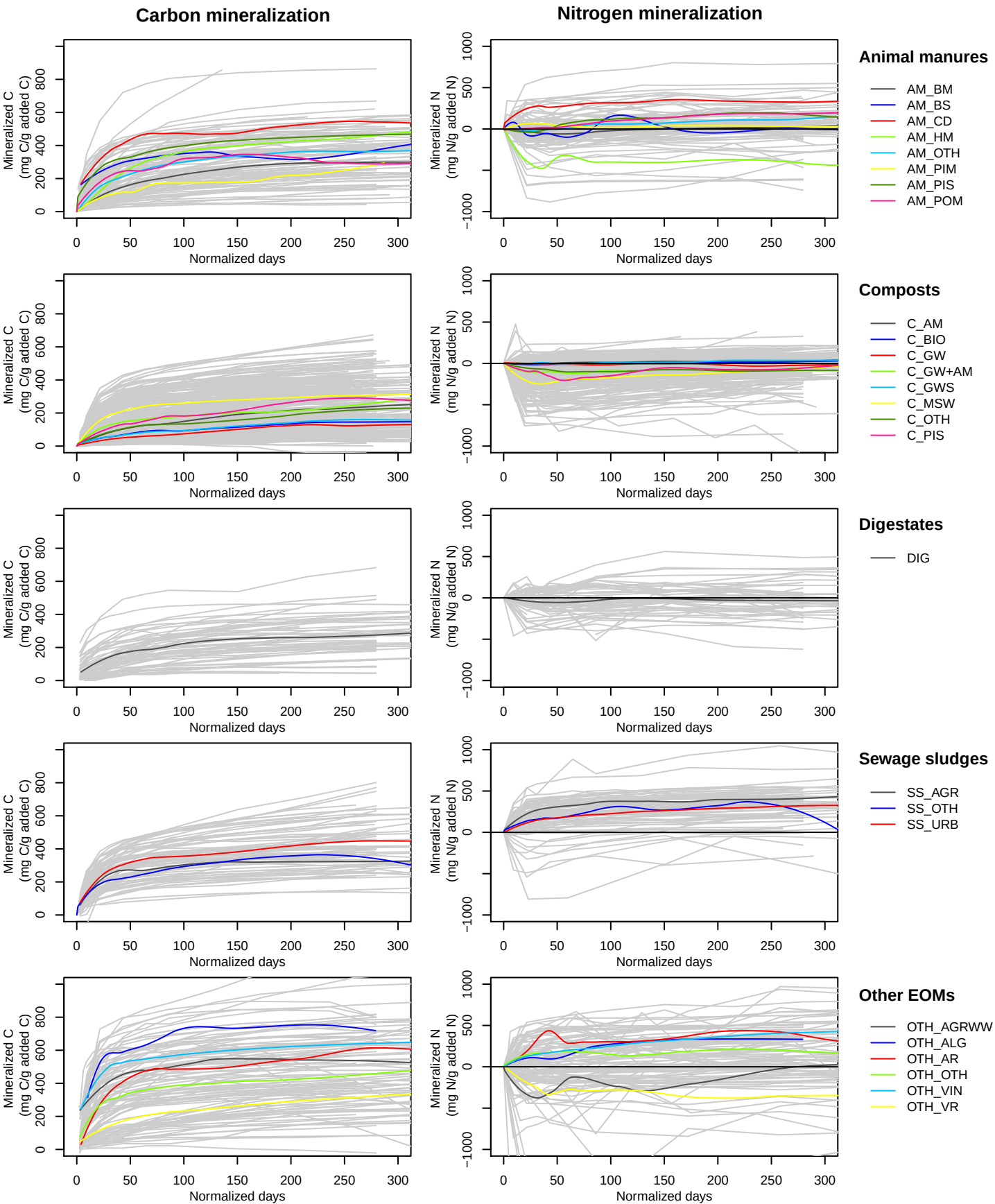
Carbon mineralization
Nitrogen mineralization
Mineralized C (mg C/g added C)
Mineralized N (mg N/g added N)
Normalized days
Animal manures
AM_BM
AM_BS
AM_CD
AM_HM
AM_OTH
AM_PIM
AM_PIS
AM_POM
Composts
C_AM
C_BIO
C_GW
C_GW+AM
C_GWS
C_MSW
C_OTH
C_PIS
Digestates
DIG
Sewage sludges
SS_AGR
SS_OTH
SS_URB
Other EOMs
OTH_AGRWW
OTH_ALG
OTH_AR
OTH_OTH
OTH_VIN
OTH_VR

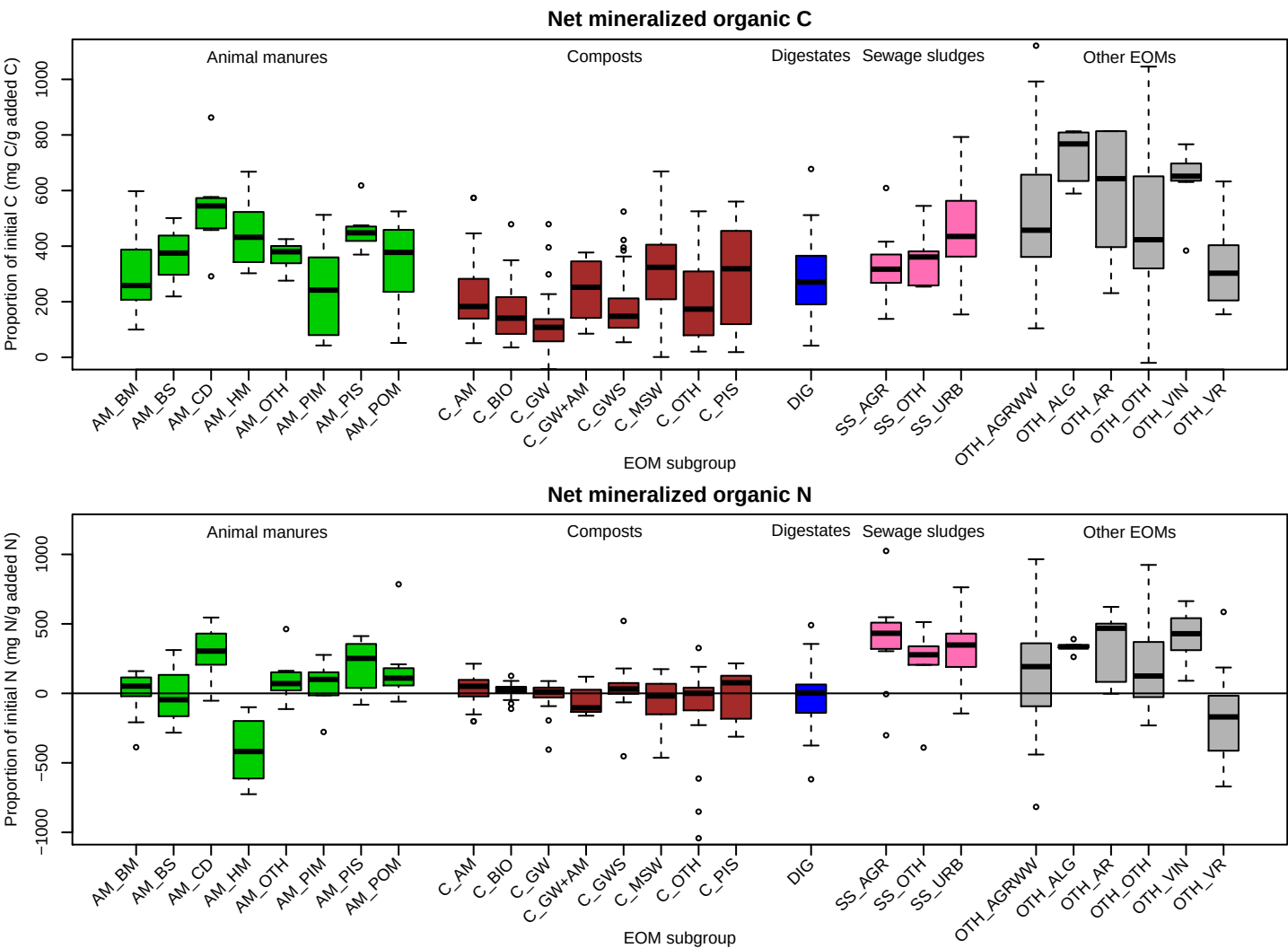
Net mineralized organic C
Animal manures
Composts
Digestates
Sewage sludges
Other EOMs
Proportion of initial C (mg C/g added C)
0
200
400
600
800
1000
AM_BM
AM_BS
AM_CD
AM_HM
AM_OTH
AM_PIM
AM_PIS
AM_POM
C_AM
C_BIO
C_GW
C_GW+AM
C_GWS
C_MSW
C_OTH
C_PIS
DIG
SS_AGR
SS_OTH
SS_URB
OTH_AGRWW
OTH_ALG
OTH_AR
OTH_OTH
OTH_VIN
OTH_VR
EOM subgroup
Net mineralized organic N
Animal manures
Composts
Digestates
Sewage sludges
Other EOMs
Proportion of initial N (mg N/g added N)
−1000
−500
0
500
1000
AM_BM
AM_BS
AM_CD
AM_HM
AM_OTH
AM_PIM
AM_PIS
AM_POM
C_AM
C_BIO
C_GW
C_GW+AM
C_GWS
C_MSW
C_OTH
C_PIS
DIG
SS_AGR
SS_OTH
SS_URB
OTH_AGRWW
OTH_ALG
OTH_AR
OTH_OTH
OTH_VIN
OTH_VR
EOM subgroup

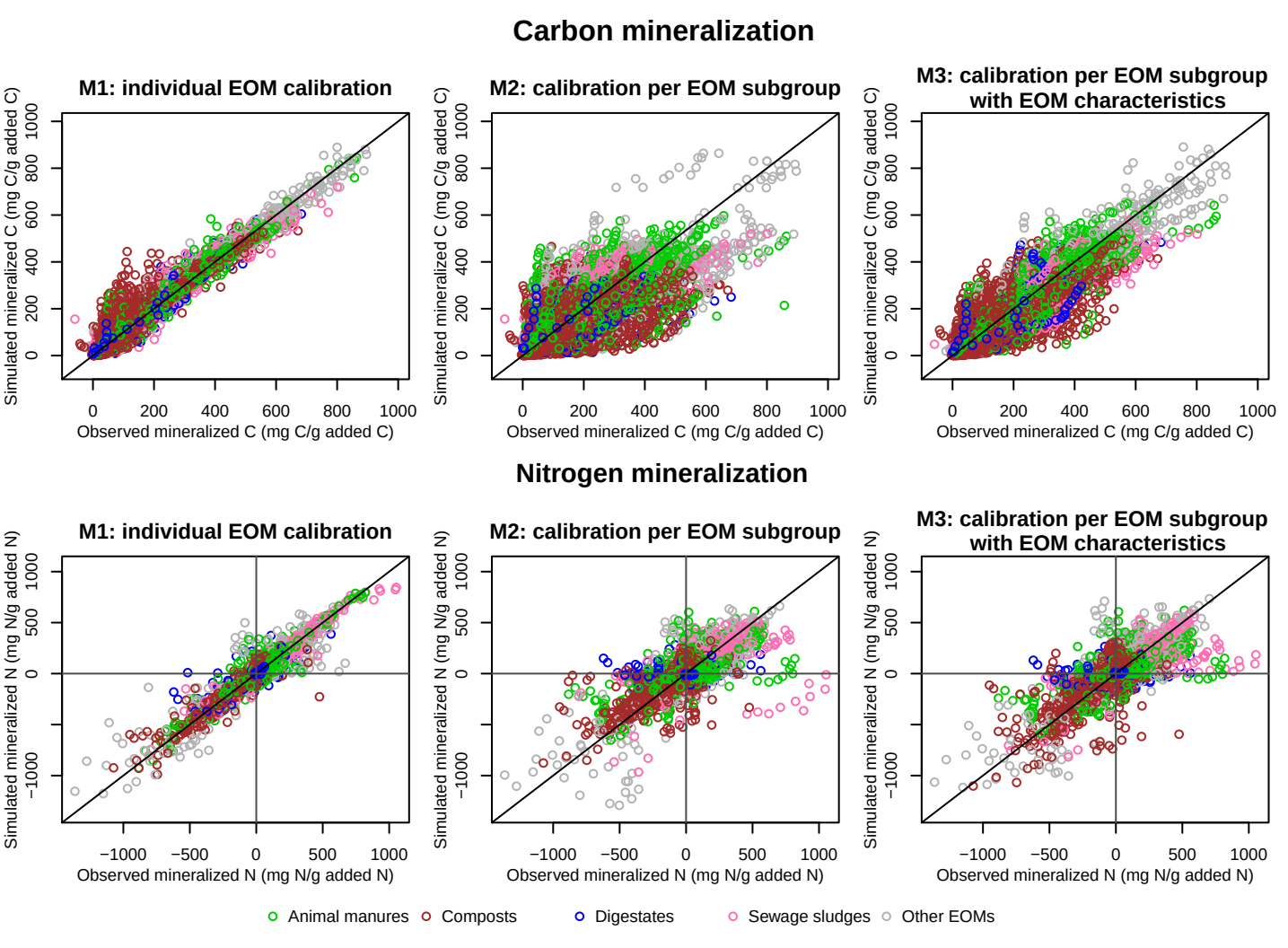
Carbon mineralization
M1: individual EOM calibration
M2: calibration per EOM subgroup
M3: calibration per EOM subgroup with EOM characteristics
Simulated mineralized C (mg C/g added C)
Observed mineralized C (mg C/g added C)
0
200
400
600
800
1000
Nitrogen mineralization
M1: individual EOM calibration
M2: calibration per EOM subgroup
M3: calibration per EOM subgroup with EOM characteristics
Simulated mineralized N (mg N/g added N)
Observed mineralized N (mg N/g added N)
−1000
−500
0
500
1000
Animal manures
Composts
Digestates
Sewage sludges
Other EOMs

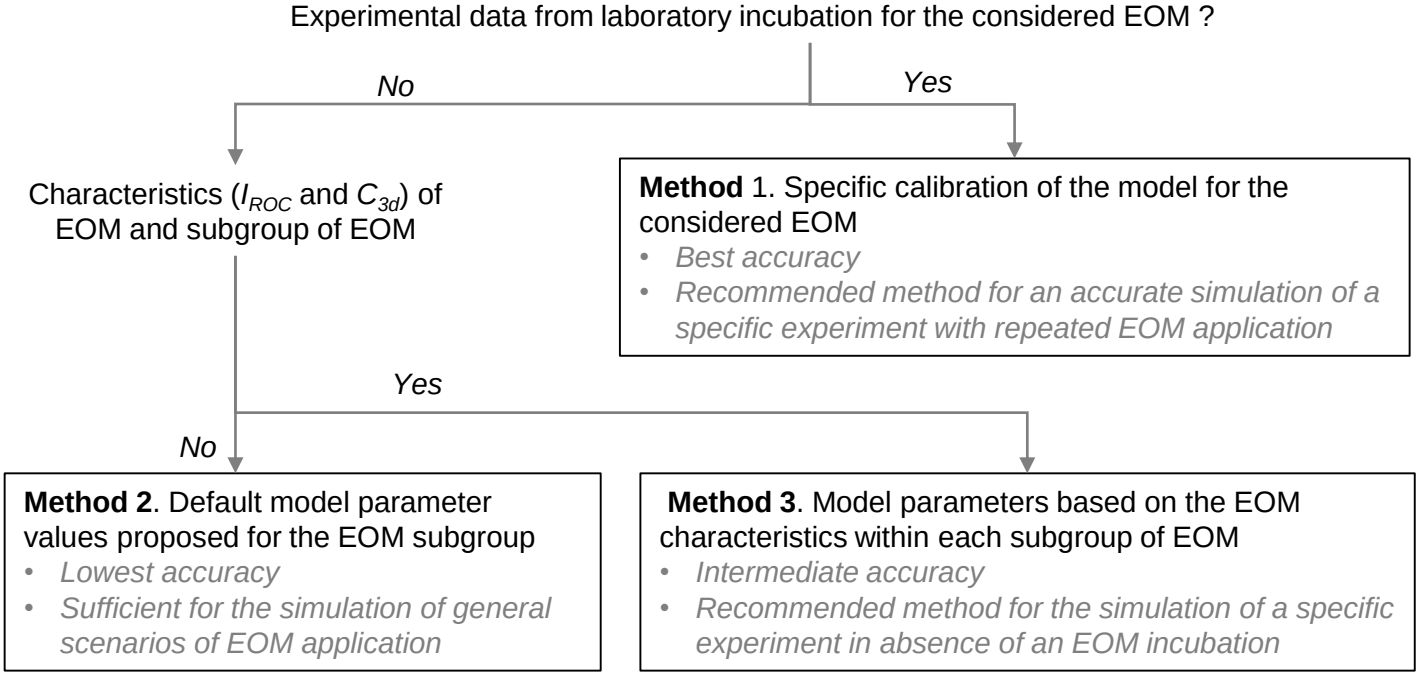
Experimental data from laboratory incubation for the considered EOM ?
No
Yes
Characteristics (I_{ROC} and C_{3d}) of EOM and subgroup of EOM
Method 1. Specific calibration of the model for the considered EOM
• *Best accuracy*
• *Recommended method for an accurate simulation of a specific experiment with repeated EOM application*
Yes
No
Method 2. Default model parameter values proposed for the EOM subgroup
• *Lowest accuracy*
• *Sufficient for the simulation of general scenarios of EOM application*
Method 3. Model parameters based on the EOM characteristics within each subgroup of EOM
• *Intermediate accuracy*
• *Recommended method for the simulation of a specific experiment in absence of an EOM incubation*